Technische Universität München

Technische Universität München
Fakultät für Elektrotechnik und Informationstechnik
Professur für Computational Photonics
Prof.Dr.-Ing. Christian Jirauschek

Coupled Transmission Line/Maxwell-Bloch Equations Approach for Electro-Optical Simulations of Terahertz Quantum Cascade Lasers

MASTER THESIS

by Longwei Zhong

April, 2017

Abstract

Quantum cascade lasers (QCLs) are compact, electrically pumped semiconductor devices, which are considered to be promising light sources for far- and mid-infrared regions. Despite its practical significance, generating ultra short pulses from QCLs by mode-locking has achieved only limited success.

There are already several successful experimental attempts by active mode locking. The purpose of this research is to build a new model based on current simulation methods to simulate mode-locking process in time domain, which would help to get a better understanding of its theoretical mechanism and redound to still unresolved issues of the field.

Acknowledgements

Thanks to Petar

I dedicate this work to my beloved mother and father

List of Symbols

Contents

1 Introduction

QCLs have gained considerable attention since they were first demonstrated at Bell Laboratories in 1994 by Jerome Faist and his colleagues[1]. Due to lack of suitable radiation sources and detectors this region remains one of the least developed spectral regions. Unlike common semiconductor lasers, which utilize electron-hole recombination to realize electromagnetic radiation, QCLs are based on intersub- band transitions in coupled quantum well superlattices[2]. Benefit from this special mechanism QCLs can utilize the electric power more efficiently and achieve a high output power.

1.1 Motivation

In the last two decades many studies have been carried out on further development as well as possible applications of QCLs. Some groups devoted themselves to improve the operation temperature, up to room temperature has been achieved[3] through special wells design of QCL structure. Some consisted on generating short pulse by using QCLs[4]. Besides, In the past few years researchers have showed high interest in the application of QCLs. There are already many ....

1.2 Related work

Mode-locking is a technique in optics, which locks multi-mode in resonant laser cavity by enforcing coherence between modes to produce extra short pulse[5]. Methods of mode-locking can be simply classified in active mode-locking (AML) and passive mode-locking(PML) depending on whether it is modulated by itself or requires external modulation source.

It has been proven to be difficult to directly employ existing techniques from the ultra fast optics community to mode-lock QCLs due to unfavorable physical effects and lack of consolidation theory about its mechanism.

1.3 Objective

2 Optical Modeling

Similar with the existing modeling methods, in this model light propagation is described with Maxwell' equation while carrier transportation is determined by Bloch equation. Without regard to lateral non-uniform distribution of electrical components due to boundaries [6, 7] QCL can be simplified to one-dimensional (1D) structure in the direction of propagation (x axis).

2.1 Light Propagation

2.2 Carrier Transport

3 Electrical Modeling

In the electrical modeling, a modified Transmission Line Method (TLM) was introduced in order to realize a dynamic modeling in time domain. TLM is a very efficient methode which is already widely used for evaluation and dynamic modeling, for example, contact resistance extraction in organic field- effect transistors [8], dynamic modeling of flow in pipelines [9] etc. However, TLM is specially for analysis of transverse electromagnetic (TEM) modes while in QCLs are transverse magnetic (TM) modes [10]. The common used metal-metal waveguide (microstrip structure) in QCLs can be regarded as quasi-TEM structure, if the substrate ($\sim$ 10 um) is thin in terms of wavelength (30 mm $\sim$ 300 mm), and if the strip conductor is very narrow ($\sim$ 50 um) in terms of wavelength, then a static analysis should be perfectly adequate.

3.1 Transmission Line Method

The conventional TLM is described by Telegrapher's equations (3.1)(3.2) with distributed components. The distributed resistance R' Under the assumptions the same with in optical modeling the simulated QCL could be regarded as a 1D nonlinear lossy transmission.
((–> to be changed: explain Distributed components: The distributed resistance R′ of the conductors is represented by a series resistor (expressed in ohms per unit length). The distributed inductance L′ (due to the magnetic field around the wires, self-inductance, etc.) is represented by a series inductor (henries per unit length). The capacitance C between the two conductors is represented by a shunt capacitor C′ (farads per unit length). The conductance G of the dielectric material separating the two conductors is represented by a shunt resistor between the signal wire and the return wire (siemens per unit length). This resistor in the model has a resistance of 1/G′ ohms.))

Telegrapher's equations:

$$\frac{\partial v(x,t)}{\partial x} = -L'\frac{\partial i(x,t)}{\partial t} - R'i(x,t) \tag{3.1}$$

$$\frac{\partial i(x,t)}{\partial x} = -C'\frac{\partial v(x,t)}{\partial t} - G'v(x,t) \tag{3.2}$$

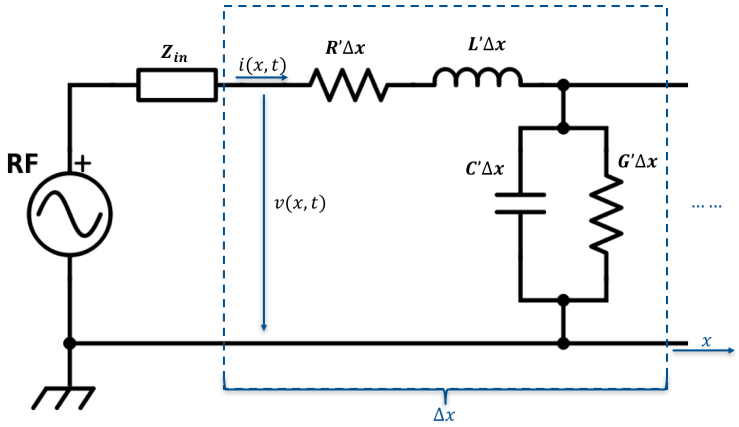

Figure 3.1: *: An equivalent circuit representation of a differential section of the waveguide with capacitance per unit length C′ and inductance per unit length L′.*

In this case, the vertical current component due to distributed conductance G′ will be replaced by current density J which was induced by carrier transmission in optical part. In order to solve these two partial differential equations, finite difference in time domain (FDTD) method was applied. This method is widely used to solve transmission line problem in time domain and has second order accuracy.

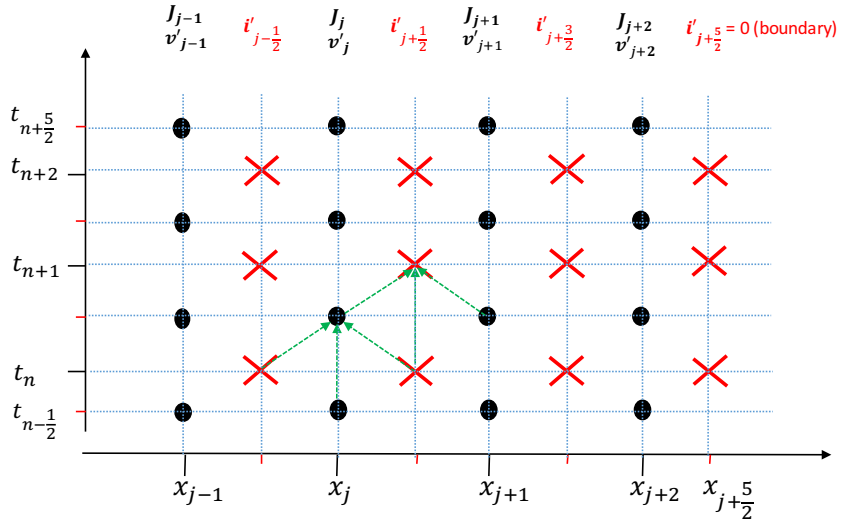

Figure 3.2: *Discretization along a staggered temporal and spatial grid.*

Following Yee's staggered grid approximation[11], voltage and current are discretized with separation of $\Delta x/2$ and $\Delta t/2$ in space and time respectively (See Figure 3.2), which leads to a second-order accurate approximation. Voltage V(x,t) and ac current i(x,t) samples are then expressed as $V\left(j*\Delta x,(n+\frac{1}{2})*\Delta t\right)$ and $i\left((j+\frac{1}{2})*\Delta x,n*\Delta t\right)$, where j and n are integers. For reasons of simplicity, in the following text they will be replaced with $V_j^{n+\frac{1}{2}}$ and $i^n_{j+\frac{1}{2}}$. After discretization, the first-order derivative of voltage

$\partial V(x,t)$ as well as current $\partial I(x,t)$ in space and time can be simply calculated with central difference method[12].

In this way the original Telegrapher's equations (3.1) and (3.2) are constructed as:

$$\frac{V_{j+1}^{n+\frac{1}{2}} - V_j^{n+\frac{1}{2}}}{\Delta x} \approx -L' \frac{i_{j+\frac{1}{2}}^{n+1} - i_{j+\frac{1}{2}}^{n}}{\Delta t} - R' i_{j+\frac{1}{2}}^{n+\frac{1}{2}} \tag{3.3}$$

$$\frac{i_{j+\frac{1}{2}}^{n} - i_{j-\frac{1}{2}}^{n}}{\Delta x} \approx -C' \frac{V_j^{n+\frac{1}{2}} - V_j^{n-\frac{1}{2}}}{\Delta t} - w\widetilde{J}_j^n \tag{3.4}$$

where, $i_{j+\frac{1}{2}}^{n+\frac{1}{2}}$ is the ac (alternating current) component of whole current and w width of simulated laser cavity. And $\widetilde{J}_j^n$ denotes ac part of current density at node j due to external RF source. Its value can be simply obtained by apply bias with or without RF source to optical modeling. The ac part of current plays a role especially in high frequency case, in which metal shows high resistance due to RF source. Besides, the last terms of equation (3.3) has to be averaged in time for sake of consistence, leading to:

$$(\frac{L'}{\Delta t} + \frac{R'}{2}) i_{j+\frac{1}{2}}^{n+1} = -\frac{V_{j+1}^{n+\frac{1}{2}} - V_j^{n+\frac{1}{2}}}{\Delta x} + (\frac{L'}{\Delta t} - \frac{R'}{2}) i_{j+\frac{1}{2}}^{n} \tag{3.5}$$

Subsequently, after rearrangement a recursive solution for Transmission line updating are explicitly expressed as:

$$i_{j+\frac{1}{2}}^{n+1} = (\frac{L'}{\Delta t} + \frac{R'}{2})^{-1} [-\frac{V_{j+1}^{n+\frac{1}{2}} - V_j^{n+\frac{1}{2}}}{\Delta x} + (\frac{L'}{\Delta t} - \frac{R'}{2}) i_{j+\frac{1}{2}}^{n}] \tag{3.6}$$

$$V_j^{n+\frac{1}{2}} = V_j^{n-\frac{1}{2}} - \frac{\Delta t}{C'\Delta x} [i_{j+\frac{1}{2}}^{n} - i_{j-\frac{1}{2}}^{n} + w\Delta x \big(J_j^n(V_j^{n-\frac{1}{2}}) - J_j^n(V_{DC})x\big)] \tag{3.7}$$

3.1.1 Boundary Conditions

Boundary conditions account for the completeness of differential equations at the boundary. In this case, the right side of QCL lefts open, so no current exists. Consequently, the boundary condition for current is $I_{end}^n = 0$.

QCL was supplied with source V_S which consists of a DC voltage source V_{DC} and an external RF source V_{RF}, therefore $V_S = V_{DC} + V_{RF}$. But due to existance of wire impedance the voltage at node 0 is not equal to source voltage V_S. The voltage source as well as wire impedance can be replaced by a Thévenin equivalent circuit consisting of an equivalent current source in series connection with an equivalent resistance. Besides, a cascading of π networks[14] is introduced for the distributed transmission line by splitting the shunt capacitance and conductance in half with two parallel capacitors and conductors at boundary, which is illustrate in Fig. 3.3.

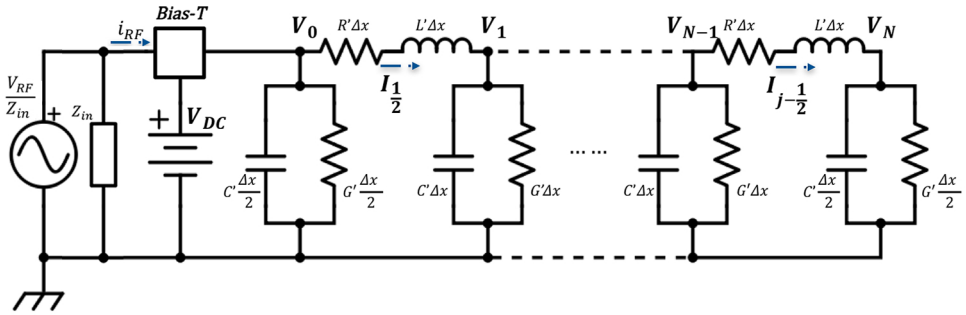

Figure 3.3: *Schematic of cascade π network representation and Thévenin equivalent circuit.*

By using Kirchhoff's current law (KCL) at node 0,

$$\frac{V_{RF}^n}{Z_{in}} = i_{\frac{1}{2}}^n + \frac{w\Delta x}{2}\widetilde{J}_0^n + C'\frac{\Delta x}{2}\frac{\partial V_0^n}{\partial t} + \frac{V_0^n - V_{DC}}{Z_{in}} \tag{3.8}$$

$$= i_{\frac{1}{2}}^n + \frac{w\Delta x}{2}\widetilde{J}_0^n + C'\frac{\Delta x}{2}\frac{V_0^{n+\frac{1}{2}} - V_0^{n-\frac{1}{2}}}{\Delta t} + \frac{V_0^{n+\frac{1}{2}} + V_0^{n-\frac{1}{2}} - 2V_{DC}}{2Z_{in}} \tag{3.9}$$

Then the equation above is rearranged to get an explicit update expression at boundary:

$$V_0^{n+\frac{1}{2}} = V_{DC} + (C'\frac{\Delta x}{2\Delta t} + \frac{1}{2Z_{in}})^{-1}[(C'\frac{\Delta x}{2\Delta t} - \frac{1}{2Z_{in}})(V_0^{n-\frac{1}{2}} - V_{DC}) - i_{\frac{1}{2}}^n - \frac{w\Delta x}{2}\widetilde{J}_0^n + \frac{V_{RF}^n}{Z_{in}}] \tag{3.10}$$

3.1.2 Initial Conditions

Adequate initial conditions play a important role as well as boundary conditions to acquire an accurate solution. However, it is really hard to determine and verify the real electrical distribution of a laser at the very beginning. Here the following initial conditions are assumed based on the current knowledge:

$$V_1^0 = V_2^0 = ... = V_j^0 ... = V_N^0 = V_{DC} \tag{3.11}$$

$$i_{\frac{1}{2}}^0 = i_{\frac{3}{2}}^0 = ... = i_{j+\frac{1}{2}}^0 ... = i_{N-\frac{1}{2}}^0 = 0 \tag{3.12}$$

where, N is the amount of grids and j integer ranging from 1 to N.

3.2 Estimation of Distributed Components

The involvement of transmission line requires distributed component parameters. Except for distributed conductance G', which will be calculated in optical part, dis-

tributed resistance R', distributed inductance L' as well as distributed capacitance C' still need to be determined. They can be either calcuted as convertial passive components (plane resistor, parallel plane capacitor and inductor), or extracted from S-Parameter, which can be directly measured with network analyser. The former methode is simple and also don't require any extra test, but could lead to large error due to neglection of fringe effect[15] as well as high frequency influence. The latter is based on experiment, so shows higher accuracy compared with former, but requires extra experiment as well as equipment, which is not always feasible for simulation research.

Distributed resistance is frequency dependent and can be obtained by measurement of S-parameter [16], which shows constant value when under certain frequency $R' = 4.5 \times 10^{-5}\sqrt{f_{RF}}$ /mm.

3.2.1 Estimation of Distributed Capacitance

The cavity of QC laser is regarded as microstrip line in this case. Quasi-TEM structures, like microstrip, will have frequency dependent impedance and effective dielectric constant. However, if the substrate ($\sim$ 10 um) is thin in terms of wavelength (30 mm $\sim$ 300 mm), and if the strip conductor is very narrow ($\sim$ 50 um) in terms of wavelength, then a static analysis should be perfectly adequate.)

Numerically, one only have to consider a small, bounded 2D region with assumption of uniform cross-section going into the page (See Figure 3.4).

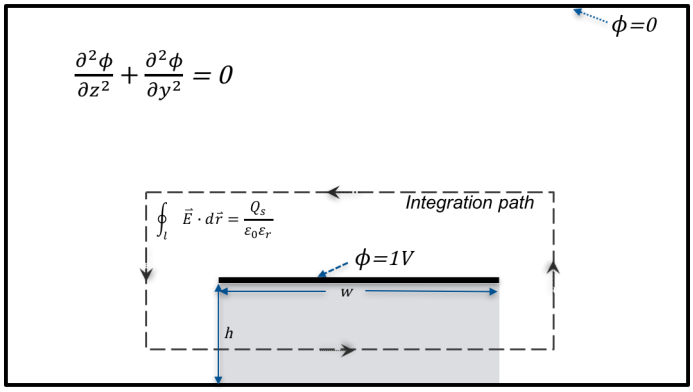

Figure 3.4: *Gauss's 2D equation.*

The electric field can be solved by Gauss's law in 2D. Solving for a strip in a box (Figure 2) the strip potential was set to 1V, the boundary to 0V and solve for the potential at a number of points inside the box. Here an electromagnetic field-solver QuickField was used which is a stand-alone software for solving partial differential equation (PDE). Figure 3 shows the calculated electric field around the strip.

$$\frac{\partial^2 \phi}{\partial y^2} = \frac{\phi_{i-1,j} - 2\phi_{i,j} + \phi_{i+1,j}}{(\Delta y)^2} \tag{3.13}$$

$$\frac{\partial^2 \phi}{\partial z^2} = \frac{\phi_{i,j-1} - 2\phi_{i,j} + \phi_{i,j+1}}{(\Delta z)^2} \tag{3.14}$$

Set $\Delta y = \Delta z = \Delta$, then spacial electrical potential at each grid except top metal layer inside box can be resolved $\phi_{i,j} = \frac{\phi_{i-1,j}+\phi_{i+1,j}+\phi_{i,j-1}+\phi_{i,j+1}}{4\Delta^2}$

3.2.2 Estimation of Distributed Inductance

4 Simulation Results and Comparison with Experiment

The simulated laser is

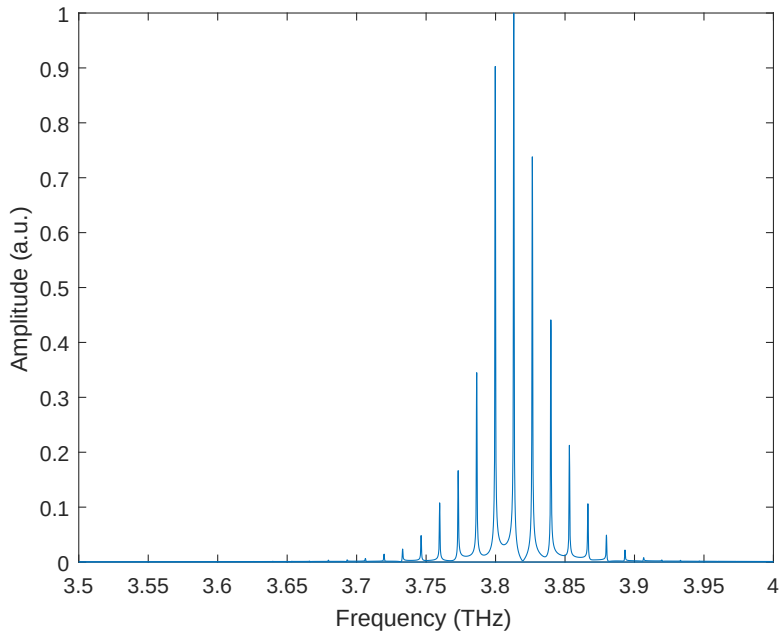

Figure 4.1: *laser spectrum.*

4.1 Simulation Setup

The source of simulated QCL consists of a DC voltage source and a RF source, which are combined through bias-T.

$$A = V_s * modA \tag{4.1}$$

$$P_{watt} = \frac{(\frac{A}{\sqrt{2}})^2}{R} = \frac{A^2}{2R} \tag{4.2}$$

$$P_{dBm} = 10 * \log_{10} \frac{P_{watt}}{1mw} = 30 + 10 * \log_{10} \frac{A^2}{2R} \tag{4.3}$$

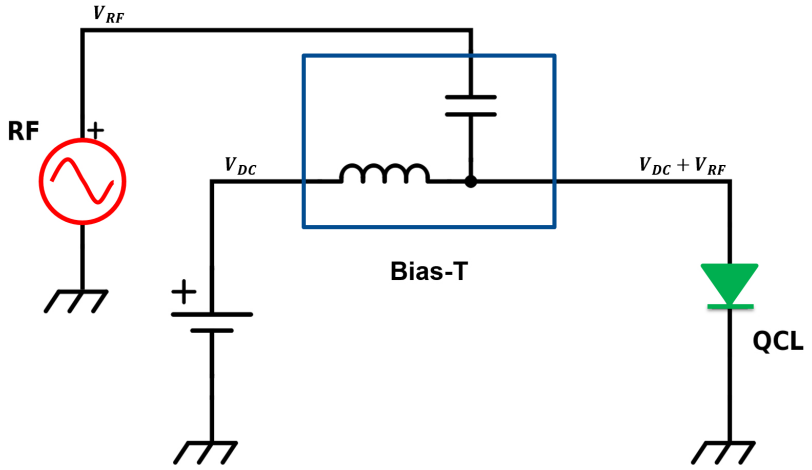

Figure 4.2: *schematic scheme.*

Table 4.1: *Simulation parameters*

Name	Symbol	Value	Unit
Cavity length	L_{tot}	3	mm
Doping density	D_p	1.5E15	cm^{-3}
Period length	L_p	54.8	nm
Overlap factor	Γ	0.8	

4.2 Simulation Setting

4.3 Simulation Results

After 100 round trips simulation, a clear short pulse was observed, as Figure 4.3 shows, from 4610 to 4690 ps in corresponding to 164 T_{rt}. Its Full Width at Half Maximum (FWHM) through this modeling is about 11.6 ps, which shows extremely good agreement with experiment result 11 ps[17].

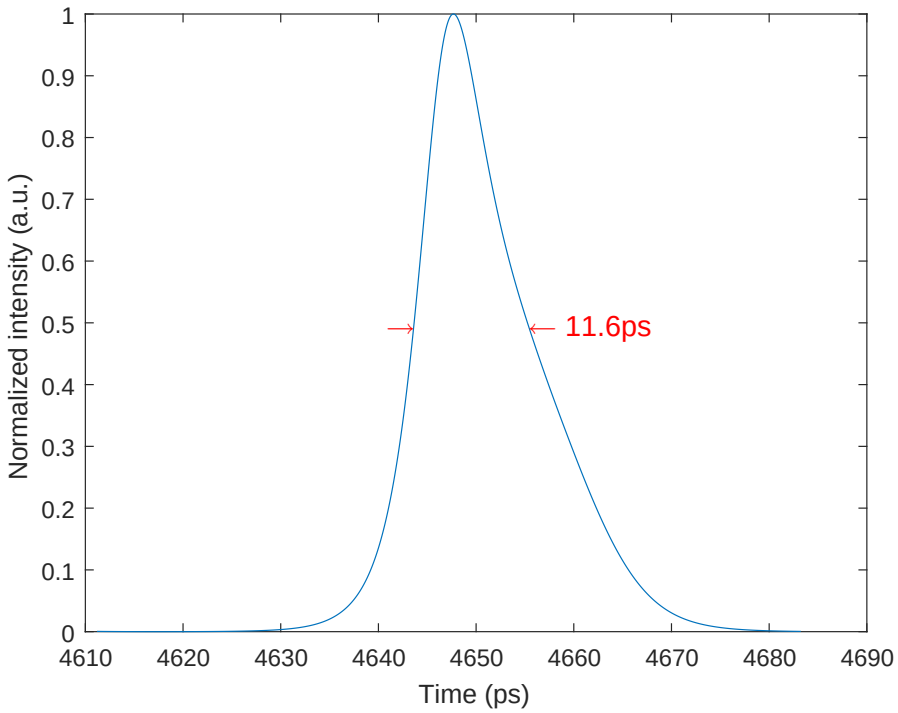

Figure 4.3: *Singel pulse from simulation.*

5 Conclusion

Bibliography

[1] J. Faist, F. Capasso, D. L. Sivco, C. Sirtori, A. L. Hutchinson, and A. Y. Cho, "Quantum cascade laser," *Science*, vol. 264, no. 5158, pp. 553–556, 1994. *Cited on page 1.*

[2] B. S. Williams, "Terahertz quantum-cascade lasers," *Nature photonics*, vol. 1, no. 9, pp. 517–525, 2007. *Cited on page 1.*

[3] Y. Bai, N. Bandyopadhyay, S. Tsao, S. Slivken, and M. Razeghi, "Room temperature quantum cascade lasers with 27% wall plug efficiency," *Applied Physics Letters*, vol. 98, no. 18, p. 181102, 2011. *Cited on page 1.*

[4] C. Y. Wang, L. Kuznetsova, V. Gkortsas, L. Diehl, F. X. Kaertner, M. A. Belkin, A. Belyanin, X. Li, D. Ham, H. Schneider, *et al.*, "Mode-locked pulses from mid-infrared quantum cascade lasers," *Optics express*, vol. 17, no. 15, pp. 12929–12943, 2009. *Cited on page 1.*

[5] H. A. Haus, "Mode-locking of lasers," *IEEE Journal of Selected Topics in Quantum Electronics*, vol. 6, no. 6, pp. 1173–1185, 2000. *Cited on page 1.*

[6] X. Huang, Y. Dikmelik, and C. Gmachl, "Non-uniform lateral current distribution in quantum cascade lasers," *Optics express*, vol. 22, no. 5, pp. 6154–6164, 2014. *Cited on page 3.*

[7] R. Dhar and D. Ban, "Nanoscopic voltage distribution of operating cascade laser devices in cryogenic temperature," *Journal of microscopy*, 2015. *Cited on page 3.*

[8] Y. Xu, R. Gwoziecki, I. Chartier, R. Coppard, F. Balestra, and G. Ghibaudo, "Modified transmission-line method for contact resistance extraction in organic field-effect transistors," *Applied Physics Letters*, vol. 97, no. 6, p. 171, 2010. *Cited on page 5.*

[9] N. Johnston, M. Pan, and S. Kudzma, "An enhanced transmission line method for modelling laminar flow of liquid in pipelines," *Proceedings of the Institution of Mechanical Engineers, Part I: Journal of Systems and Control Engineering*, vol. 228, no. 4, pp. 193–206, 2014. *Cited on page 5.*

[10] C. Yan, Q. J. Wang, L. Diehl, M. Hentschel, J. Wiersig, N. Yu, C. Pflügl, F. Capasso, M. A. Belkin, T. Edamura, *et al.*, "Directional emission and universal far-field

behavior from semiconductor lasers with limaçon-shaped microcavity," *Applied Physics Letters*, vol. 94, no. 25, p. 251101, 2009. *Cited on page 5.*

[11] K. Yee, "Numerical solution of initial boundary value problems involving maxwell's equations in isotropic media," *IEEE Transactions on antennas and propagation*, vol. 14, no. 3, pp. 302–307, 1966. *Cited on page 6.*

[12] D. Yang, P. Tong, and X. Deng, "A central difference method with low numerical dispersion for solving the scalar wave equation," *Geophysical Prospecting*, vol. 60, no. 5, pp. 885–905, 2012. *Cited on page 7.*

[13] S. D. Gedney, "Introduction to the finite-difference time-domain (fdtd) method for electromagnetics," *Synthesis Lectures on Computational Electromagnetics*, vol. 6, no. 1, pp. 1–250, 2011. *No citations.*

[14] A. Orlandi and C. R. Paul, "Fdtd analysis of lossy, multiconductor transmission lines terminated in arbitrary loads," *IEEE Transactions on Electromagnetic Compatibility*, vol. 38, no. 3, pp. 388–399, 1996. *Cited on page 7.*

[15] K. Pillai, "Fringing field of finite parallel-plate capacitors," in *Proceedings of the Institution of Electrical Engineers*, vol. 117, pp. 1201–1204, IET, 1970. *Cited on page 9.*

[16] W. Maineult, L. Ding, P. Gellie, P. Filloux, C. Sirtori, S. Barbieri, T. Akalin, J.-F. Lampin, I. Sagnes, H. Beere, *et al.*, "Microwave modulation of terahertz quantum cascade lasers: a transmission-line approach," *Applied Physics Letters*, vol. 96, no. 2, p. 021108, 2010. *Cited on page 9.*

[17] P. Gellie, S. Barbieri, J.-F. Lampin, P. Filloux, C. Manquest, C. Sirtori, I. Sagnes, S. P. Khanna, E. H. Linfield, A. G. Davies, *et al.*, "Injection-locking of terahertz quantum cascade lasers up to 35ghz using rf amplitude modulation," *Optics express*, vol. 18, no. 20, pp. 20799–20816, 2010. *Cited on page 12.*